

Emplacement and cooling of komatiite lavas

Herbert E. Huppert*, R. Stephen J. Sparks†, J. Stewart Turner‡
& Nicholas T. Arndt§

* Department of Applied Mathematics and Theoretical Physics, University of Cambridge, Silver Street, Cambridge CB3 9EW, UK

† Department of Earth Sciences, University of Cambridge, Cambridge CB2 3EQ, UK

‡ Research School of Earth Sciences, Australian National University, Canberra, A.C.T. 2601, Australia

§ Max-Planck-Institut für Chemie, Saarstrasse 23, Postfach 3060, D-6500 Mainz, FRG

We propose that komatiite lavas were emplaced as turbulent flows, accompanied by vigorous forced convection with cooling rates often in excess of hundreds of °C h⁻¹. They melted and assimilated up to 10% of the ground over which they flowed, forming deep channels. Nickel sulphide mineralization may have resulted from incorporation of sulphur-rich sediment. After emplacement, high cooling rates persisted, resulting in spinifex textures due to compositional convection.

KOMATIITES are believed to represent ultramafic liquids which erupted at temperatures of 1,400–1,700 °C with estimated viscosities in the range 0.1–1 Pa s, and with MgO contents of 18–35%^{1–3}. Such lavas are mostly of Archaean age. They indicate that thermal conditions of the early Earth were significantly different from those of today and provide insights into the composition of the Archaean mantle. They commonly exhibit spectacular spinifex textures and internal layering⁴, and some are also the host to important nickel sulphide mineralization⁵. Interpretation of their chemical compositions, petrological and geological features and mineralization requires an understanding of their eruption, emplacement and cooling. As a contribution to this understanding, we present both a fluid dynamical analysis of the flow and cooling of komatiites and experimental studies which simulate the formation of spinifex texture in ponded komatiite lavas.

Recent basalts have eruption temperatures usually below 1,250 °C and viscosities > 50 Pa s; almost all of them flow by laminar shear at low Reynolds number and cool by conduction. We propose that, because of their much lower viscosities, komatiites would have flowed turbulently at high Reynolds number, and would have cooled initially by forced convection. We suggest that, after emplacement, komatiite lavas still cooled rapidly by thermal convection and demonstrate, by experimental studies on cooling of saturated aqueous solutions, that convective effects can strongly influence the development of the characteristic spinifex textures.

Magma ascent

Magma ascends to the surface because of its buoyancy^{6,7}. At high Reynolds number, Re , the two-dimensional discharge rate, Q , from a long fissure of width d can be estimated as

$$Q = \left(\frac{g\Delta\rho}{k\rho_m} \right)^{1/2} d^{3/2} \quad (1)$$

where g is gravity, $\Delta\rho$ is the assumed constant density difference

between the magma and the lithosphere overlying its source, ρ_m is the magma density, k is a friction coefficient which can assume values between ~0.01 and 0.06 depending on the surface roughness of the fissure⁷, and the Reynolds number is

$$Re = Q/\nu \quad (2)$$

where ν is the kinematic viscosity. In principle, in order to account for the density variation in the lithosphere, the compressibility of the melt and the tortuous nature of the fissure, a more elaborate treatment than that leading to equation (1) is required. However, the accuracy of equation (1) is sufficient for our calculations. At shallow depths in the lithosphere, the value of $\Delta\rho$ is ~300 kg m⁻³, whereas at depths of 100 km the value of $\Delta\rho$ has been estimated as 100 kg m⁻³ (ref. 8).

Table 1 gives the values of Q , flow velocity $v = Q/d$, and Re for a plausible range of natural fissure widths. The komatiite is assumed to have a viscosity of 0.3 Pa s, a density of 2,800 kg m⁻³ and we have set $\Delta\rho$ to a conservative value of 100 kg m⁻³. The value of 0.03 has been used for the friction coefficient. Table 1 shows that even for the narrowest fissure (0.3 m), Re greatly exceeds the critical value (equal to ~2,000) required for turbulent flow. Komatiites are thus likely to have flowed turbulently up the fissure before eruption. This should be compared with the largest historic eruptions of basalts, for which Q and Re are less than 10 m² s⁻¹ and 600 respectively⁷.

Lava emplacement

A fundamental feature of a turbulent flow is that the heat transfer is much greater than in a laminar flow, where heat is lost entirely by conduction. In turbulent flows, mixing maintains a uniform temperature throughout the span of the flow and greatly increases heat transfer to the surroundings. Thus, in turbulent komatiite flows the ground surface would be quickly heated up to temperatures of 1,600–1,700 °C. In greenstone belts, komatiites often flow over rocks, such as tholeiitic basalt and sediment^{9,10}, which have substantially lower melting temperatures. We suggest that komatiites could have melted and assimilated this underlying rock.

Our model, a geometric sketch of which is presented in Fig. 1, is related to that proposed by Hulme^{11,12}, who argued that the sinuous rilles on the Moon were caused by thermal erosion of lava channels by turbulent lunar flows. We consider flow on a shallow slope beneath a deep body of water. Both floor rocks and water have initial temperature T_0 , which is taken to be 0 °C. The heat transfer from the komatiite, due to forced, turbulent convection, melts some of the ground which is then

Table 1 The two-dimensional flow rate, Q , the vertical velocity, v , and the Reynolds number, Re in a fissure of width d

d (m)	Q (m ² s ⁻¹)	v (m s ⁻¹)	Re
0.3	0.56	1.9	5.2×10^3
1.0	3.4	3.4	3.2×10^4
3.0	17.8	5.9	1.6×10^5
10.0	108	10.8	1.0×10^6

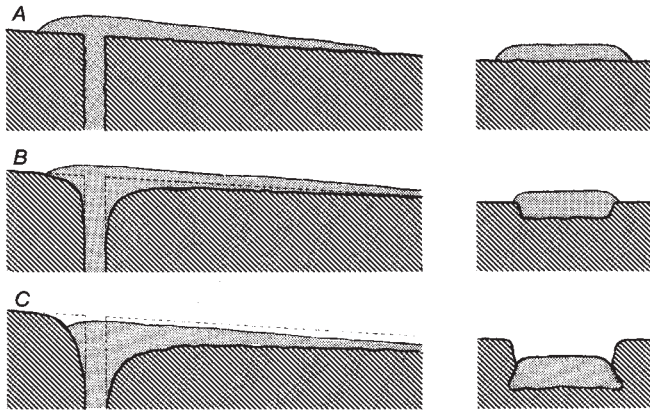


Fig. 1 Longitudinal and cross-sectional sketches of the fissure and lava flow showing the melting of the ground and the formation of an erosional channel with time.

assimilated. Efficient cooling by the water above the flow forms a thin crust on top of the lava and prevents any mixing between the two. As the lava cools, crystals form within it, which decreases the rate of cooling. The komatiite is assumed to flow in the form of a gravity current of high Reynolds number over a slope which is sufficiently small that its effects can be neglected. The thickness of the current, h , can then be determined¹³ by

$$h = (\frac{1}{2}Q^2\rho_l/g\delta\rho)^{1/3} \quad (3)$$

where $\delta\rho$ represents the density difference ($1,800 \text{ kg m}^{-3}$) between the komatiite and seawater. Table 2 presents the flow thickness, velocity, u , and Reynolds number for different values of Q . A gravity current with a Reynolds number greater than ~ 500 is fully turbulent¹⁴. The values in Table 2 indicate that this is the case for all komatiite flows.

At steady state the melting rate is given by^{11,15}

$$\frac{dS}{dt} = \frac{H}{\rho_g[c_g(T_m - T_0) + L_g]} \quad (4)$$

where H is the heat transfer rate to the ground, ρ_g is the density of the ground, c_g is the specific heat of the ground, T_m is both the melting temperature of the ground and the solidification temperature of the komatiite and L_g is the heat of fusion of the ground. The heat transfer is related to T_1 , the lava temperature, and T_m through a heat transfer coefficient, h_T , by¹⁵

$$H = h_T(T_1 - T_m) \quad (5)$$

An approximation to the heat transfer coefficient can be obtained by modifying empirical relationships for turbulent pipe flows¹⁵. This leads to

$$h_T = 0.018 \frac{k_l}{h} Pr^{0.4} Re^{0.8} \quad (6)$$

where k_l is the lava conductivity and Pr its Prandtl number.

Table 2 shows that transfer coefficients of between 500 and $1,000 \text{ W m}^{-2} \text{ }^\circ\text{C}^{-1}$ result for flow rates in the range 0.5–

Table 2 Lava flow thickness, h , its velocity, u , the Reynolds number, Re , the heat transfer coefficient, h_T , and the coefficient modified by crystallization, h_T^* , as a function of Q

$Q(\text{m}^2 \text{ s}^{-1})$	$h(\text{m})$	$u(\text{m s}^{-1})$	Re	h_T ($\text{W m}^{-2} \text{ }^\circ\text{C}^{-1}$)	h_T^* ($\text{W m}^{-2} \text{ }^\circ\text{C}^{-1}$)
0.5	0.27	1.8	4.7×10^3	498	238
1	0.43	2.3	9.3×10^3	543	259
10	1.99	5.0	9.3×10^4	739	353
100	9.26	10.8	9.3×10^5	1,000	477

Table 3 The cooling rate at the source, $\dot{T}(0)$, the erosion rate at the source, $\dot{S}(0)$, and the length scale over which the temperature of the lava decreases, D^{-1} , as a function of Q

$Q(\text{m}^2 \text{ s}^{-1})$	$\dot{T}(0) (\text{ }^\circ\text{C h}^{-1})$	$\dot{S}(0) (\text{m per day})$	$D^{-1} (\text{km})$
1	1,300 (2,730)	3.33 (6.98)	2.9 (1.4)
10	280 (590)	3.33 (6.98)	28.5 (13.6)
100	61 (127)	3.33 (6.98)	285 (136)

The second entry, in parentheses, is the value if latent heat effects are set equal to zero.

$100 \text{ m}^2 \text{ s}^{-1}$. This variation in the heat transfer coefficient is fairly small and for simplicity we have taken $h_T = 750 \text{ W m}^{-2} \text{ }^\circ\text{C}^{-1}$ in the subsequent calculations. With the values of physical parameters listed below inserted into equations (4) to (6), the melting rate of the ground near the source is calculated to be $8.1 \times 10^{-5} \text{ m s}^{-1}$ (7 m per day), confirming that thermal erosion was a major effect during the emplacement of komatiites. (The physical parameters used were: $k_l = k_c = 1 \text{ W m}^{-1} \text{ }^\circ\text{C}^{-1}$; $c_l = c_g = 730 \text{ J kg}^{-1} \text{ }^\circ\text{C}^{-1}$; $\rho_l = 2,800 \text{ kg m}^{-3}$; $\rho_g = 2,700 \text{ kg m}^{-3}$; $L_g = L_x = 5 \times 10^5 \text{ J kg}^{-1}$; $T_0 = 0 \text{ }^\circ\text{C}$; $T_m = 1,200 \text{ }^\circ\text{C}$; $T_1(x=0) = 1,600 \text{ }^\circ\text{C}$; $\theta_0 = T_1(x=0) - T_m = 400 \text{ }^\circ\text{C}$; and $Pr = 219$.)

A thin crust forms at the contact with seawater. At the top of the crust the temperature is T_0 , while at the bottom it is T_m . The crustal thickness, a , is determined from the fact that in a steady state the conductive heat transfer through the crust equals the heat transfer from the lava given by equation (5). Thus

$$a = k_c(T_m - T_0)/h_T(T_1 - T_m) \quad (7)$$

where k_c is the conductivity of the crust. Near the source $a \approx 4 \text{ mm}$ and increases away from the source as the lava temperature decreases.

Cooling of the lava

Heat loss from the lava causes crystallization, which releases latent heat, L_x . A quantitative heat budget calculation indicates that the lava temperature as a function of downstream distance x is given by

$$T_1 = T_m + \frac{D\theta_0}{(E\theta_0 + D)e^{Dx} - E\theta_0} \quad (8)$$

where θ_0 is the difference between the temperature of the lava at source and the melting temperature of the ground, $D = 2h_T^*/(\rho_l c_l Q)$,

$$E = \frac{h_T^*}{Q\rho_g[c_g(T_m - T_0) + L_g]} \quad (9)$$

and

$$h_T^* = \frac{h_T}{1 - L_x x'(T)/c_l} \quad (10)$$

with $x'(T) = -\frac{1}{625} \text{ }^\circ\text{C}^{-1}$ representing the rate of change of crystal fraction with temperature¹⁶. For $Q = 10 \text{ m}^2 \text{ s}^{-1}$, the lava temperature as a function of distance is plotted in Fig. 2A. The temperature decreases with a length scale given by D^{-1} , which is evaluated for other flow rates in Table 3. If the lava increases the ground temperature to T_m but does not melt it, its temperature is given by $T_1 = T_m + \theta_0 e^{-Dx}$, also plotted in Fig. 2A.

The cooling rates of the lava flow for $Q = 10 \text{ m}^2 \text{ s}^{-1}$ are plotted in Fig. 2B; one curve incorporates latent heat release due to crystallization while the other does not. With latent heat effects the cooling rate is $280 \text{ }^\circ\text{C h}^{-1}$ near the source and decreases steadily away from it. Initial cooling rates for other flow rates are given in Table 3.

These calculations assume that crystallization occurs in thermodynamic equilibrium, although experimental studies^{17,18} on magnesian-rich basic melts show that rapid cooling rates can

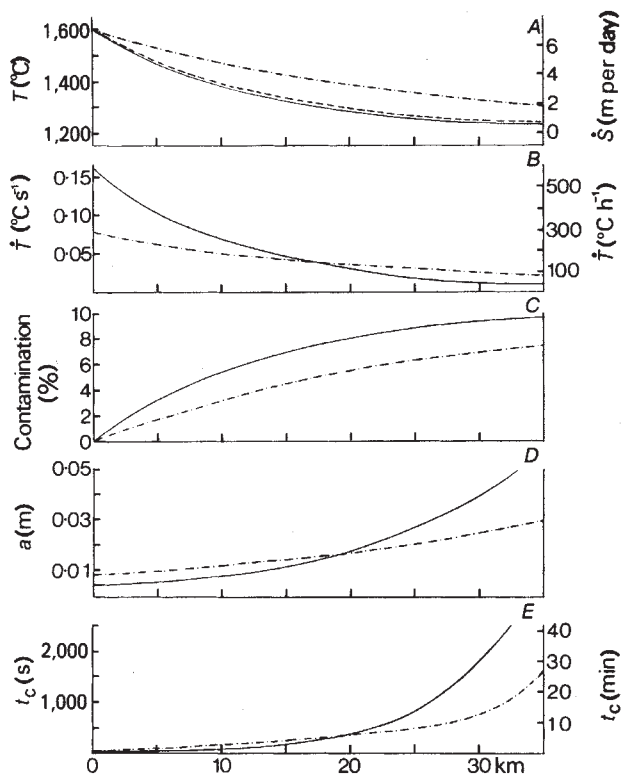


Fig. 2 A, The temperature of the lava, T , and the erosion rate of the ground, S . —, With melting; ---, without melting. B, The cooling rate; C, the percentage of contamination; D, the crustal thickness, a ; and E, the time scale for the crust to form; all as a function of distance from the source. In A–E the dot-dash (·-·) line incorporates the latent heat release due to crystal formation, while the solid line omits this effect ($L = 0$).

cause large undercoolings. Extrapolation of Donaldson's experimental data¹⁸ to cooling rates of several hundreds of °C per hour suggests undercoolings of 50–70 °C. The cooling rates in excess of 10^3 °C h⁻¹, for small Q , might result in considerable delays in olivine nucleation, with the extreme case of zero crystallization. Table 3 shows the results of calculations neglecting crystallization completely; cooling rates and melting rates increase as the undercooling increases.

As the melting rate of the ground is proportional to $T_1 - T_m$, it has the same functional form as T_1 (Fig. 2A). Our calculations indicate that one hour after eruption, with the flow rate $Q = 10 \text{ m}^2 \text{ s}^{-1}$, the channel depth at source would be 14 cm, while 15 km from the source it would be 8 cm. After a week the depth at source would be 23 m and 15 km from source it would be 13 m. If no crystallization occurred, the depths would be just over twice these values. If the lava flow were 250 m wide, the volume erupted after one hour and one week would be 9×10^6 and $1.5 \times 10^9 \text{ m}^3$, respectively. These volumes are comparable to small- and medium-sized basalt eruptions.

Assimilation of the melted ground contaminates the lava, as indicated in Fig. 2C. The contamination rises steadily to an asymptotic value of 10.4%, independent of the flow rate, and could significantly change the trace element and isotopic composition of the lava, although it would have only minor effects on the major element composition.

The crustal thickness, given by equation (7) and plotted in Fig. 2D, is of the order of a few centimetres, consistent with the geological evidence that komatiites often show an upper quench glassy zone of this magnitude⁴. The time scale for this crust to grow (Fig. 2E) is quite short and indicates that if at any time

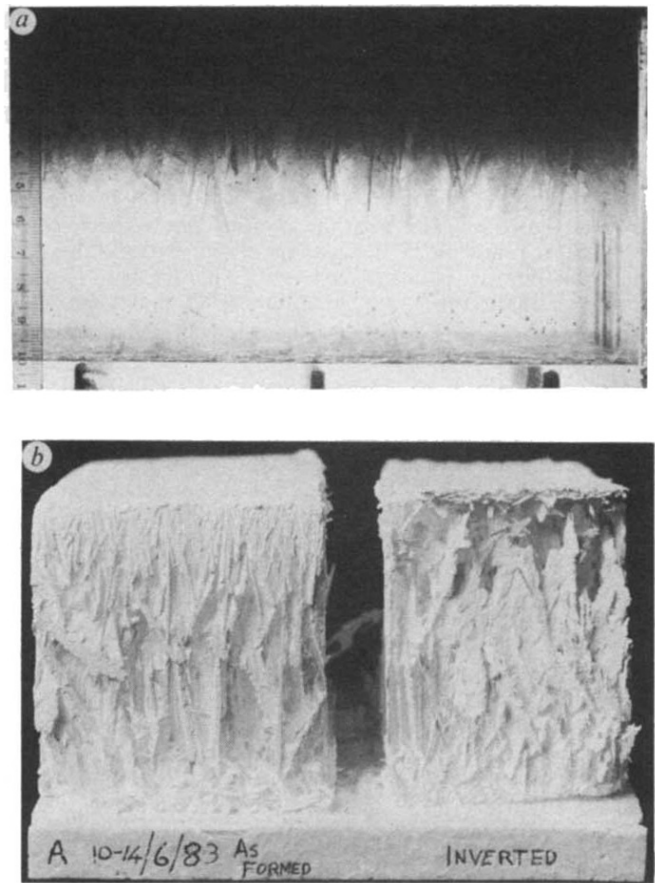


Fig. 3 Photographs of an experiment in which aqueous Na_2CO_3 was cooled from above. a, Photograph with back-lighting after 1 h 38 min. Note the growth of long crystals with nearly vertical orientation, followed by a layer of eutectic with a sharp horizontal boundary. The scale on the left indicates the distance (in cm) from the cooled roof. b, The subsequent crystal block after ice was allowed to melt and run out of the upright (left) and inverted (right) halves of the block.

the crust is broken up by the turbulent flow beneath it and falls into the flow, a new crust forms fairly rapidly. Thus a steady-state crust caps the flow during almost all the emplacement period.

Post-emplacement processes

Once the supply of magma has ceased, the komatiite can be expected to drain into any available depressions, which would include the channel incised by thermal erosion. In many lavas only part of the cooling will have been accomplished during active flow and the ponded lava will continue to cool and crystallize. If the crust is thin, theoretical calculations (which will be presented in detail elsewhere) show that the ponded komatiite will continue to cool by thermal convection. By balancing the conductive heat flux across the crust with the convective flux in the interior, we obtain initial cooling rates of tens to hundreds of °C per hour. As the crust thickens from being a few centimetres thick, the lava temperature decreases and eventually turbulent convection will decrease in vigour. At this stage the heat budget is dominated by a balance between the conductive flux across the crust and latent heat release. We envisage that granular olivines suspended in the lava will now fall out to form the peridotitic cumulate layer, typical of the lower parts of many komatiites¹⁰.

In order to simulate the development of spinifex texture, we crystallized saturated aqueous solutions by cooling from above. Figure 3 shows the results of cooling an aqueous solution of

12.3% anhydrous Na_2CO_3 in a cubical container initially at 31 °C by circulating alcohol at -30 °C through the top plate. Initially, vigorous thermal convection occurred and small dendritic crystals of hydrated Na_2CO_3 nucleated on the roof. At first the crystals showed a wide range of orientations with respect to the roof (Fig. 3a). As the experiment progressed, however, the crystals increasingly became oriented perpendicular to the roof (Fig. 3b). At the same time, a stagnant pool of less dense, residual fluid formed between the growing crystals due to compositional convection¹⁹. The tips of the crystals extended beyond this layer into the saturated, convecting fluid beneath. Experiments on other saturated solutions of Na_2SO_4 and KNO_3 mirrored these features, confirming that the general behaviour is not dependent on composition.

Geological interpretations

Our analysis shows that komatiites can become significantly contaminated by assimilation of the underlying rock (Fig. 2C). We emphasize three points concerning the contamination process. First, floor rocks will be quickly melted and efficiently mixed into the turbulent flow. Xenoliths would not be expected to survive. Second, the chemical signature of contamination would not be extreme; only elements strongly concentrated in the contaminant and depleted in the komatiite would be noticeably affected, and the evidence for this would be most apparent in measurements of the ratios of elements with different compatibilities. Third, the amount of contamination is strongly dependent on flow conditions and distance downstream. As most eruptions probably fluctuate in intensity, the amount of contamination is likely to be very variable even within one flow. Non-systematic variations with indices of olivine fractionation would be anticipated for those elements that are sensitive indicators of contamination.

An application of the thermal erosion model relates to the origin of nickel sulphide mineralization, which we suggest could have been formed by komatiites melting underlying sulphur-rich sediments. Contamination of 10% of a sediment containing 6% sulphur could increase the sulphur content of the lava by 0.6%. The sulphur forms an immiscible sulphide liquid which extracts nickel from the komatiite and segregates to the base of the flow⁵. The sulphide liquid could separate effectively even from the turbulently flowing lava because of its high density (~4,500 kg m⁻³), especially if it coagulated to form large drops with high settling velocities.

At Kambalda in Western Australia, the nickel sulphide ores are found at the base of komatiite flows where the lavas are thickest⁹. The long linear depressions which the ores occupy have been interpreted as pre-existing features down which the lavas were channelled. However, it would then be expected that sediment would accumulate in the channels and be thickest in these areas, whereas sediment rarely underlies the thickest komatiite flows and nickel sulphide is present there instead²⁰.

This antithetic relationship between the occurrence of sediment and ore is consistent with the suggestion that the

depressions are thermal erosion channels where the lava has digested the sediment and cut into underlying basalt. The model also avoids the problem of trying to explain why highly magnesian melts carry such high contents of sulphur²⁰. Thus, this model explains many of the features of mineralization, such as the regional association of sediment and ore-bearing komatiites, evident throughout the Western Australia nickel province. It remains to be seen, however, whether the model is of more general applicability.

Our work also relates to the origin of the characteristic textures and layering of komatiite flows²¹. Skeletal olivine morphologies and mineralogical peculiarities, such as crystallization of clinopyroxene, appear to demand either high rates of cooling or melts undercooled by hundreds of °C^{17,18,22}. Cooling rates, based on conductive models²³, are orders of magnitude less than the rates required by experimental studies of olivine growth^{17,18}. Thus, it is difficult to see how the slow cooling rates characteristic of conductive models can cause these textures. Our analysis of the post-emplacement phase, combined with Donaldson's experimental results¹⁷, indicates that rapid cooling rates and large undercoolings can be achieved. Our experiments also indicate that compositional convection can significantly influence the morphology of crystals growing from the roof. Skeletal and dendritic crystal morphologies and metastable crystallization could be a consequence of both thermal and compositional convection.

Our study suggests that during flow, high cooling rates cause either pre-existing phenocrysts to grow, or high nucleation rates. Granular equant olivines remain suspended during turbulent flow and initially on emplacement, when thermal convection might occur. As convective stirring diminishes in vigour, the olivines settle out to form a cumulate layer. Olivine crystals nucleate on the roof and at first grow as dendrites in many orientations. However, compositional convection causes a pool of differentiated melt to form between the crystals beneath the roof. As the pool develops, the tips of olivine crystals grow preferentially at the margins, as in the experiment, and the olivines increasingly grow perpendicular to the roof.

We conclude that komatiites probably flowed turbulently and cooled in part by convection. One consequence of this behaviour is that komatiites can melt and assimilate underlying rock to form deep thermal erosion channels. Assimilation of sulphur-rich sediments may result in the formation of nickel ore deposits. After emplacement, komatiites can continue to cool by thermal convection. Nucleation of crystals on the roof results in the development of spinifex texture. All these processes have important influences on the development of the characteristic geology, textures, geochemistry and mineralization of these rocks.

We acknowledge useful comments by I. H. Campbell, C. H. Donaldson, R. Kerr, R. W. Nesbitt, L. Wilson and G. Worster. Our research on komatiites, stimulated during visits to the Research School of Earth Sciences during 1982, is supported by a grant from the BP Venture Research Unit to H.E.H. and R.S.J.S.

Received 22 November 1983; accepted 15 February 1984.

- Viljoen, M. J. & Viljoen, R. P. *Spec. Publ. geol. Soc. S. Afr.* **2**, 87-112 (1969).
- Arndt, N. T. & Nisbet, E. G. (eds) in *Komatiites* Ch. 2, 19-26 (Allen & Unwin, London, 1982).
- Bickle, M. J. in *Komatiites* (eds Arndt, N. T. & Nisbet, E. G.) Ch. 27, 479-494 (Allen & Unwin, London, 1982).
- Donaldson, C. H. in *Komatiites* (eds Arndt, N. T. & Nisbet, E. G.) Ch. 16, 213-244 (Allen & Unwin, London, 1982).
- Naldrett, A. J. *Econ. Geol.* **74**, 1520-1528 (1979).
- Elder, J. W. *Geothermal Systems* (Academic, New York, 1982).
- Wilson, L. & Head, J. W. *J. geophys. Res.* **86**, 2971-3001 (1981).
- Nisbet, E. G. & Walker, D. *Earth planet. Sci. Lett.* **60**, 103-113 (1982).
- Leshner, C. M., Lee, R. F., Groves, D. I., Bickle, M. J. & Donaldson, M. J. *Econ. Geol.* **76**, 1714-1728 (1981).
- Arndt, N. T., Naldrett, A. J. & Pyke, D. R. *J. Petrol.* **18**, 319-369 (1977).
- Hulme, G. *Modern Geol.* **4**, 107-117 (1973).
- Hulme, G. *Geophys. Surv.* **5**, 245-279 (1982).
- Britter, R. E. & Simpson, J. E. *J. Fluid Mech.* **88**, 223-240 (1978).
- Simpson, J. E. & Britter, R. E. *J. Fluid Mech.* **94**, 477-495 (1979).
- Holman, J. P. *Heat Transfer* (McGraw Hill, New York, 1976).
- Bickle, M. J. *Prog. exp. Petrol.* **4**, 187-195 (1978).
- Donaldson, C. H. *Contr. Miner. Petrol.* **57**, 187-213 (1976).
- Donaldson, C. H. *Contr. Miner. Petrol.* **69**, 21-32 (1979).
- Chen, C. F. & Turner, J. S. *J. geophys. Res.* **85**, 2573-2593 (1980).
- Gresham, J. J. & Loftus-Hills, G. D. *Econ. Geol.* **76**, 1373-1416 (1981).
- Pyke, D. R., Naldrett, A. J. & Eckstrand, O. R. *Bull. geol. Soc. Am.* **84**, 955-978 (1973).
- Campbell, I. H. & Arndt, N. T. *Geol. Mag.* **119**, 605-610 (1982).
- Usselman, T. M., Hodge, D. S., Naldrett, A. J. & Campbell, I. H. *Can. Miner.* **17**, 361-372 (1979).